Collagen Organization in Canine Myxomatous Mitral Valve Disease: An X-Ray Diffraction Study

Mojtaba Hadian,* Brendan M. Corcoran,† Richard I. Han,† J. Günter Grossmann,‡ and Jeremy P. Bradshaw*
*Veterinary Biomedical Sciences, Royal (Dick) School of Veterinary Studies, University of Edinburgh, Summerhall, Edinburgh EH9 1QH, United Kingdom; †Hospital for Small Animals, Veterinary Clinical Sciences, Easter Bush Veterinary Centre, University of Edinburgh, Roslin Midlothian EH25 9RG, United Kingdom; ‡Science and Technology Facilities Council Daresbury Laboratory, Daresbury Science and Innovation Campus, Warrington WA4 4AD, United Kingdom

ABSTRACT Collagen fibrils, a major component of mitral valve leaflets, play an important role in defining shape and providing mechanical strength and flexibility. Histopathological studies show that collagen fibrils undergo dramatic changes in the course of myxomatous mitral valve disease in both dogs and humans. However, little is known about the detailed organization of collagen in this disease. This study was designed to analyze and compare collagen fibril organization in healthy and lesional areas of myxomatous mitral valves of dogs, using synchrotron small-angle x-ray diffraction. The orientation, density, and alignment of collagen fibrils were mapped across six different valves. The findings reveal a preferred collagen alignment in the main body of the leaflets between two commissures. Qualitative and quantitative analysis of the data showed significant differences between affected and lesion-free areas in terms of collagen content, fibril alignment, and total tissue volume. Regression analysis of the amount of collagen compared to the total tissue content at each point revealed a significant relationship between these two parameters in lesion-free but not in affected areas. This is the first time this technique has been used to map collagen fibrils in cardiac tissue; the findings have important applications to human cardiology.

INTRODUCTION

The mitral or left atrioventricular valve of the heart lies between the left atrium and the left ventricle and prevents backflow to the left atrium during ventricular systole. The mitral valve has two leaflets, namely the mural and the aortic (Fig. 1). Normally the leaflets are thin, translucent, and soft, although during disease processes a set of different pathological and morphological changes may occur. Tendinous cords attach the leaflets to two closely arranged groups of papillary muscles. Myxomatous mitral valve disease (MMVD) is the most common acquired cardiac disease of dogs. It is a disease of significant veterinary importance and also of emerging comparative interest. It is usually known as mitral valve prolapse in humans. The condition is typified by the loss of mechanical integrity of the valve leaflets, failure of proper coaptation of the leaflet edges during ventricular systole, mitral valve regurgitation, and, in a significant proportion of affected dogs, left-sided congestive heart failure (1–3).

The etiopathogenesis of acquired MMVD is poorly understood in both dogs and humans, and there is little information about alteration of collagen in canine MMVD, in particular regarding changes in the spatial distribution of collagen fibrils in the valves. Thus, greater knowledge of collagen structure is a necessary step in the course of understanding the disease processes. Moreover, tissue engineering and bioartificial valves are rapidly burgeoning areas that would benefit from detailed information about heart valve structure. The purpose of this study was to determine the changes in collagen fibril organization between diseased and healthy areas of valve leaflets using the technique of small-angle x-ray diffraction. X-ray diffraction has the advantage over electron microscopy that the tissue is maintained during the x-ray exposure so that prior chemical processing of the tissue is eliminated. Furthermore, unlike electron microscopy, which examines a very localized volume of tissue, x-rays pass through the entire the sample thickness, and the results thus represent averages throughout the tissue.

MATERIAL AND METHODS

Mitral valve leaflets were collected from five confirmed affected dogs and one healthy control. All tissue samples were frozen within 10 min of collection. In addition to the control sample, because diseased and normal areas coexist in one leaflet, each valve could also be used as its own control.

X-ray diffraction measurements

Collagen molecules lie almost parallel to the fibril axis and diffract x-rays from the 670 Å repeating pattern of gap and overlap regions. The intensity of diffraction is related to the amount of collagen, and the alignment of the diffraction pattern reflects the alignment of the fibers. Therefore, diffraction patterns can be used to probe the alignment of the collagen fibrils that produced that diffraction. The technique can also be used to determine total tissue content (collagenous and noncollagenous) by quantitative analysis of total x-ray scattering at any point (4–6).

X-ray diffraction measurements were performed with synchrotron radiation (Experimental Station 2.1, Synchrotron Radiation Source, The Council for the Central Laboratory of the Research Councils (CCLRC), Daresbury, UK) using a method developed from that of Aghamohammadzadeh and co-workers (4). Briefly, specimens were mounted in a specially designed

Submitted April 3, 2007, and accepted for publication May 30, 2007.

Address reprint requests to Mojtaba Hadian, Veterinary Biomedical Sciences, Royal (Dick) School of Veterinary Studies, University of Edinburgh, Summerhall, Edinburgh EH9 1QH, UK. Tel.: 44-131-650-6142; Fax: 44-131-650-6511; E-mail: m.hadian@ed.ac.uk.

Editor: Marcia Newcomer.

0006-3495/07/10/2472/05 $2.00

doi: 10.1529/biophysj.107.107847

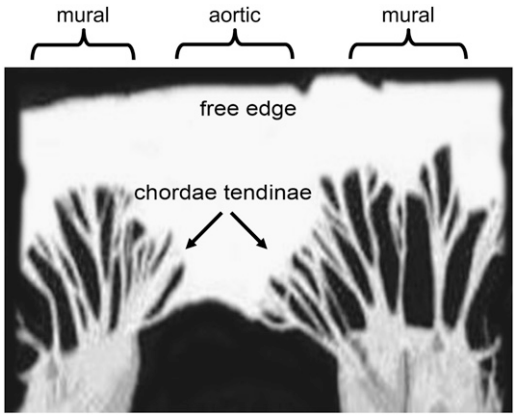

FIGURE 1 A normal canine mitral valve spread open by cutting through the mural leaflet.

sample cell and attached to a movable sample stage. The stage was programmed to translate in a raster of 1-mm steps, horizontally and vertically, while a finely focused (0.1 mm vertical × 1 mm horizontal) beam of 1.54 Å wavelength x-rays recorded the fiber diffraction pattern for 45 s at each point. Each sample was typically measured at 300 points, in a grid of 20 × 15 pixels. A multiwire two-dimensional area detector, placed 4 m from the sample, collected the diffraction data. The collection of diffraction data and movement of the sample relative to the beam were coordinated by a computer running a Python (www.python.org) script file. Calibration measurements included the detector response, in which the efficiency of each pixel was determined by a long exposure to a randomly decaying radioactive source, and detector calibration, which used the well-characterized diffraction pattern of wet rat tail collagen.

Data analysis

The diffraction pattern of a fibrous material, such as collagen, contains information in the meridional plane, describing structure along the axis of the fiber, and in the equatorial plane, describing lateral structure. For this study, Bragg reflections of the meridional diffraction pattern were recorded and analyzed to provide information about the collagen content and the degree and prevailing angle of alignment of the fibrils. The level of background scattering was also determined to give an indication of the amount of noncollagen tissue. Data analysis was performed using the program FiberFix (Collaborative Computational Project for Fiber Diffraction and Solution Scattering, CCP13). A ring was defined, centered on the middle of the diffraction pattern and wide enough to encompass the third, fourth, and fifth orders of meridional diffraction (Fig. 2). This region was chosen because it was sufficiently clear of any x-ray scattering from the backstop but included strongly diffracting Bragg peaks. The third and fifth orders of diffraction are characteristically very bright for type I collagen and have excellent signal/noise ratios, thereby simplifying the tasks of background subtraction and peak shape analysis. PeakFit (Version 4, AISN Software) was used to fit Gaussian peaks to the annular distribution of scattering intensity (Fig. 3). The Gaussians were then analyzed in terms of peak area (total diffracted intensity of the selected area of the diffraction pattern, related to the amount of collagen), peak center (angle of preferred fibril orientation), peak width (degree of fibril alignment), and mean background level (related to the amount of nonordered material). These values were then plotted to produce maps of each parameter across each valve leaflet.

Statistical analysis

The numerical diffraction values of total issue density, collagen fibril density, and degree of collagen alignment were analyzed separately for each leaflet using a two-sample *t*-test to compare affected and lesion-free areas. Significant differences were taken at $p < 0.05$. Analysis of regression was carried out to determine whether there was any relationship between amount of collagen and total tissue density in diseased and lesion-free areas.

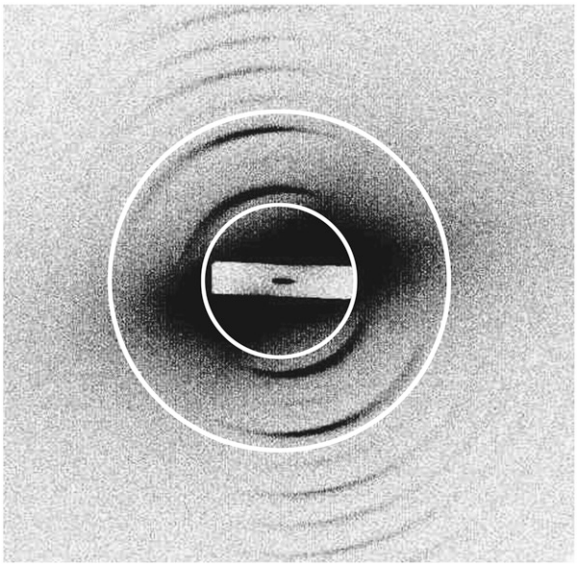

FIGURE 2 A representative x-ray diffraction pattern from canine mitral valve collagen. The pattern is dominated by a series of meridional Bragg reflections, arising from constructive diffraction of x-rays by the regularly repeating 670 Å axial structure of collagen fibrils within the sample. X-ray diffraction measurements were performed using synchrotron radiation (Experimental Station 2.1, Synchrotron Radiation Source, CCLRC, Daresbury, UK). The superimposed circles define a ring encompassing the third, fourth, and fifth Bragg peaks of meridional diffraction. Circular integration of diffracted intensity in this region was used to provide quantitative information on the amount of collagen fibrils and their orientation.

RESULTS

A typical small-angle x-ray diffraction pattern from a dog mitral valve leaflet is shown in Fig. 2. The x-ray beam passed

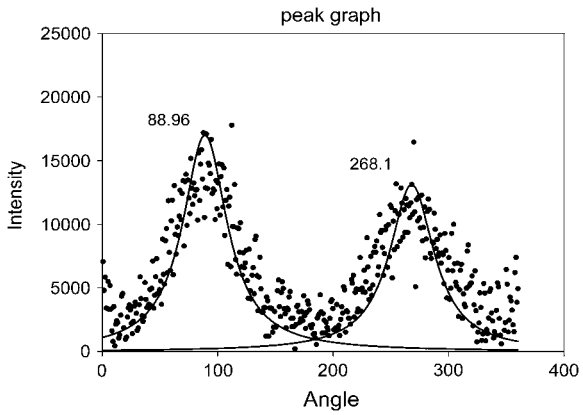

FIGURE 3 The annular distribution of diffracted intensity from canine mitral valve collagen. The data result from circular integration as described in the text and Fig. 2. Horizontal axis, angle; vertical axis, intensity (arbitrary units). Also shown is a pair of fitted Gaussian distributions centered at 88.96° and 268.1°.

through the sample perpendicular to the plane of the leaflet. Because collagen fibrils can occur in all possible orientations within this plane, the diffraction pattern may appear as a series of concentric circles. The anisotropic distribution (Fig. 3) of intensity in this example reveals a preferred angle of orientation of the fibrils.

Estimation of total tissue

Highly ordered material, such as collagen, produces a well-defined diffraction pattern, which overlays an anisotropic background of x-ray scattering by any disordered material that the x-ray beam strikes. A sensitive measure of the amount of tissue (collagenous and noncollagenous) at any one point on the leaflet is provided by the quantitative analysis of this noncoherent scattering of x-rays. Absorption of the x-ray beam by the sample can also be estimated by comparing the current measured at ion chambers before and behind the sample. A regression analysis of the two methods for one of our samples showed that they are closely related (>95% significance), thereby validating our approach. Total tissue density differed significantly ($p < 0.05$) between affected and lesion-free areas. The contour maps of the diseased samples (an example is given in Fig. 4 *A*) also revealed a considerable variation in total tissue content distribution among diseased and unaffected areas that was not consistent with a specific pattern.

Collagen fibril orientation

Fig. 4 *B* illustrates a map of collagen fibril orientation across a single leaflet. In the visibly normal areas of the midzone of the leaflets, the collagen fibrils run parallel to the free edge, meaning they take up a transverse course between two commissures. However, when they approach the edge of leaflets close to the annulus, they become oriented more vertically, such that they are orthogonal to the adjacent areas. In diseased areas, which are mostly located on the free margins of the

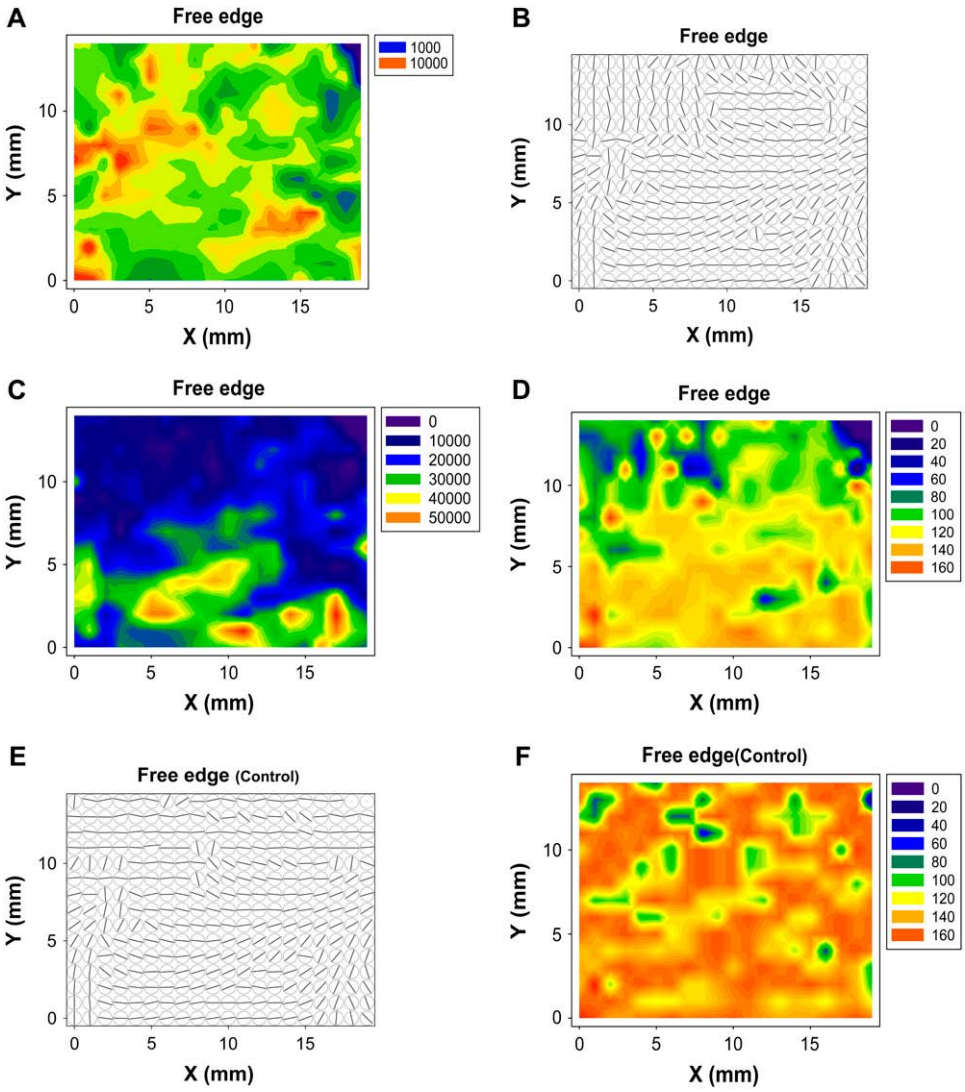

FIGURE 4 Contour maps showing an area of 20 × 15 mm of a single canine mitral valve leaflet. (*A*) Total (noncollagenous) tissue density, determined from the background (incoherent) x-ray scattering in a ring centered on the middle of the diffraction pattern and enclosing the third, fourth, and fifth meridional Bragg peaks. The background was measured in a region of reciprocal space that contained no diffraction features from collagen fibrils. Preferred orientation of collagen fibrils in diseased (*B*) and apparently healthy (*E*) mitral valve leaflets, determined by fitting Gaussian distributions to the Bragg peaks and determining the angular position of the peak center. The major difference between normal and diseased valves is in the free margins of the leaflets, where the disordered collagen fibrils of the diseased valve contrast starkly with the well-aligned fibrils of normal tissue. Collagen fibril density (*C*), determined from the total area under the Bragg peaks (total diffracted intensity). Degree of alignment of collagen fibrils in diseased (*D*) and apparently healthy (*F*) valve leaflets, determined from the width of the fitted Gaussian distributions. For ease of comparison with the other plots, the data are expressed as $180° - W$, where W is the full width at half height (in degrees) of the Gaussian distribution. Note that free edges of the leaflets are the locations where lesions are usually found. The healthy valve (*F*) displays a remarkable degree of alignment across the entire leaflet.

leaflets, the orientations of fibrils are haphazard. This contrasts with healthy regions and healthy valve (Fig. 4 *E*), where the direction of fibrils is more or less continuous with the fibrils in neighboring chordae tendineae and there is an ordered pattern of collagen fibrils across the valve.

Collagen fibril density

Fig. 4 *C* is a representative plot of collagen fibril density, determined on the basis of the strength of collagen diffraction at each point. These plots were derived from two different fibril populations: those with a preferred orientation and those without. This plot therefore shows the total diffraction irrespective of fibril orientation and so represents directly the relative amount of collagen fibers in the path of the x-ray beam. In all samples, the total diffraction, and therefore the amount of collagen, significantly increased ($p < 0.05$) from the diseased free edge of the leaflet to the unaffected base of the valves.

Degree of collagen alignment

Plots were drawn to map the degree of preferred alignment of the collagen fibrils. All the diseased leaflets showed nonuniform distribution of collagen alignment, with clear differences in the degree of preferential alignment between the diseased and healthy areas. These differences were consistent in all samples, and, as illustrated by Fig. 4 *D*, it was clear that the maximally aligned collagen is located toward the lesion-free periphery of the leaflets ($p < 0.05$). A comparison of these affected regions with the same areas in apparently healthy leaflets (Fig. 4 *F*) is a clear indication of the effect the disease has on collagen fibril alignment.

DISCUSSION

We have shown that small-angle x-ray diffraction may be used to study the different characteristics of the axially projected structure of collagen fibrils in myxomatous mitral valve. We have applied this technique to determine the various attributes of collagen fibrils in the diseased canine mitral valves and here present detailed maps of collagen fibril orientation, collagen density, the degree of alignment of the fibrils, and the relative amount of tissue density. This allows us to understand better the spatial arrangements of collagen within diseased valves. Any changes that affect the quality, quantity, or organization of collagen could lead to the mechanical failure and dysfunction of mitral valves.

The identification of collagen fibril orientation is one of the most striking findings of this study and shows that the mass of preferentially aligned collagen runs differently in different regions. In the main lesion-free body of the leaflets, collagen has a transverse course between the commissures. Near the free edge, it is almost a continuation of the collagen fibrils in the chordae tendineae. Because fiber orientation is the most effective way to optimize strength without increasing weight, fiber direction tends to reflect the prevalent tensile forces acting on a tissue (7). Therefore, knowledge of pattern of fibril alignment would have important implications for mechanical, bioprosthetic, and tissue-engineered valves and may inform the design of mitral valve substitutes. In contrast, diseased areas showed no distinct preferred orientation, and the collagen fibrils were disorganized with a haphazard and irregular arrangement. This confirmed what was previously suspected from histopathological and transmission electron microscopy studies (8).

In other tissue types dynamic changes in collagen alignment can occur in response to continuous mechanical force, but the short time frame of valve leaflet movement is unlikely to allow collagen fibrils to rearrange in response to changes in force alone. In MMVD, which is an age-related disease, the alignment of fibrils declines, whereas in aged specimens of other tissues, collagen tends to have the best-defined patterns, which indicates a greater degree of regularity from increased cross-linking of the collagen molecules (9). This suggests that the collagen changes that occur with MMVD are not simply an aging process.

The quantity of collagen was also greatly reduced in the affected areas compared to nonaffected areas. Because the tensile strength of collagen fibrils is directly proportional to the mass of the fibrils, it can be assumed that the affected areas will be less capable of resisting the load and strain imposed by ventricular systole. The free edge of normal leaflets is the thickest part of the leaflet (10), and in healthy valves, collagen content is related to tissue thickness. The plots of baseline scattering in this study showed notable variation across the leaflets, which did not correspond to diseased areas. Regression analysis of the amount of collagen compared to the total tissue content at each pixel ($p \leq 0.01$, $n = 120$ points) revealed that there was significant relationship between these two parameters in lesion-free areas. However, this relationship did not hold true in affected areas, where depletion of collagen is not reflected in a parallel decline in total tissue content. One possible explanation is that MMVD involves increased production and deposition of glycosaminoglycans (GAGs). The different types of GAGs have diverse properties for absorbance and for destructive and constructive interference (1), and although some of them could produce a clear and ordered diffraction pattern, others would only contribute to tissue density. It is also believed that GAGs in the right proportions do play a role to maintain collagen fibrils in specific spatial order. Thus, the increasing amount of the GAGs would not only disturb that spatial order but, by reducing the physical space, might also encourage the process of collagen depletion. Furthermore, determining the exact types of concerned GAGs as another step forward in understating of the disease is suggested. An additional confounding factor is that the type of collagen present in connective tissues is linked to the type and quantity of related GAGs. Type III collagen tends to

be associated with more GAGs, although there are conflicting reports on the changes in Type III collagen content in human myxomatous mitral valve disease (9,11), and the exact makeup of collagen types in canine MMVD still needs to be determined.

This work was supported by the CCLRC, the Cavalier King Charles Spaniel Club, and the Kennel Club. Mojtaba Hadian is sponsored by Iran Ministry of Science. The authors would like to thank Kalotina (Tina) Geraki for her technical support.

REFERENCES

1. Kittleson, M. D. 1998. Myxomatous atrioventricular valvular degeneration. *In* Small Animal Cardiovascular Medicine. M. D. Kittleson and R. D. Kienle, editors. Mosby, St. Louis. 297–318.
2. Pedersen, H. D., and J. Haggstrom. 2000. Mitral valve prolapse in the dog: a model of mitral valve prolapse in man. *Cardiovasc. Res.* 47: 234–243.
3. Van Vleet, J. F., and V. J. Ferrans. 2001. Cardiovascular system. *In* Thomson's Special Veterinary Pathology. M. D. McGavin, W. W. Carlton, and J. F. Zachary, editors. Mosby, St. Louis. 211–213.
4. Aghamohammadzadeh, H., R. H. Newton, and K. M. Meek. 2004. X-ray scattering used to map the preferred collagen orientation in the human cornea and limbus. *Structure.* 12:249–256.
5. Meek, K., and A. J. Quantock. 2001. The use of x-ray scattering techniques to determine corneal ultrastructure. *Prog. Retin. Eye Res.* 20: 95–137.
6. Miller, A., J. P. Bradshaw, E. Y. Jones, R. D. Fraser, T. P. MacRae, and E. Suzuki. 1985. The structure of collagen. *Ciba Found. Symp.* 114:65–79.
7. Sellaro, T. L. 2003. Effects of collagen orientation on the medium-term fatigue response of heart valve biomaterials. Dissertation. School of Engineering, University of Pittsburgh, Pittsburgh.
8. Tamura, K., Y. Fukuda, M. Ishizaki, Y. Masuda, N. Yamanaka, and V. J. Ferrans. 1995. Abnormalities in elastic fibers and other connective-tissue components of floppy mitral valve. *Am. Heart J.* 129:1149–1158.
9. James, V. J., J. F. McConnell, and M. Capel. 1991. The d-spacing of collagen from mitral heart valves changes with ageing, but not with collagen type III content. *Biochim. Biophys. Acta.* 1078:13–22.
10. Ho, S. Y. 2002. Anatomy of the mitral valve. *Heart.* 88:iv5–iv10.
11. Hammer, D., C. V. Leier, N. Baba, J. S. Vasko, C. F. Wooley, and S. R. Pinnell. 1979. Altered collagen composition in a prolapsing mitral valve with ruptured chordae tendineae. *Am. J. Med.* 67:863–866.